

Electronic Supplementary Information

Coaxial Nickel Cobalt Selenide/Nitrogen-doped Carbon Nanotube Array as a Three-Dimensional Self-Supported Electrode for Electrochemical Energy Storage

Chen Zhang^{1,*}, Shang Wang,² Junwu Xiao²

¹College of Petroleum Equipment and Electrical Engineering, Dongying Vocational Institute,
Dongying, PR China

²Key Laboratory of Material Chemistry for Energy Conversion and Storage, Ministry of Education,
Hubei Key Laboratory of Material Chemistry and Service Failure, Department of Chemistry and
Chemical Engineering, Huazhong University of Science and Technology, Wuhan 430074, China

E-mail: dychenzhang@gmail.com

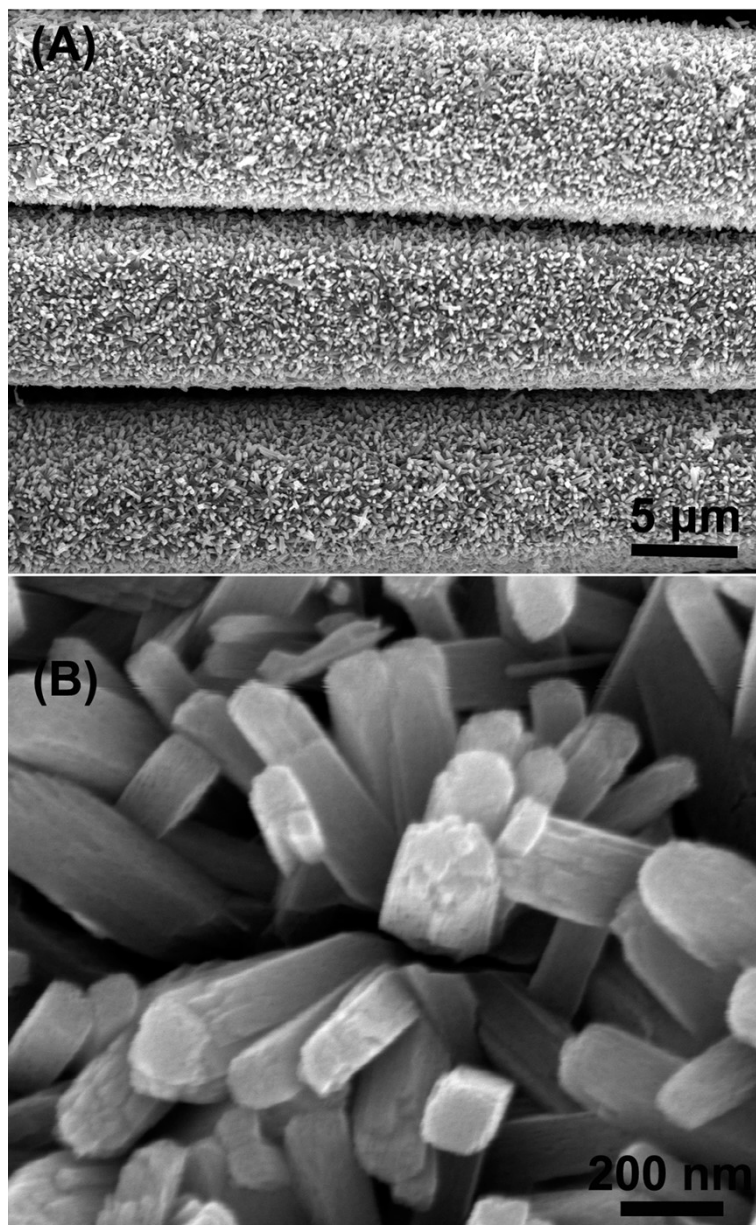


Figure S1. (A) Low and (B) high magnified SEM images of FeOOH nanoarray grown on carbon fiber paper via a hydrolysis of FeCl₃.

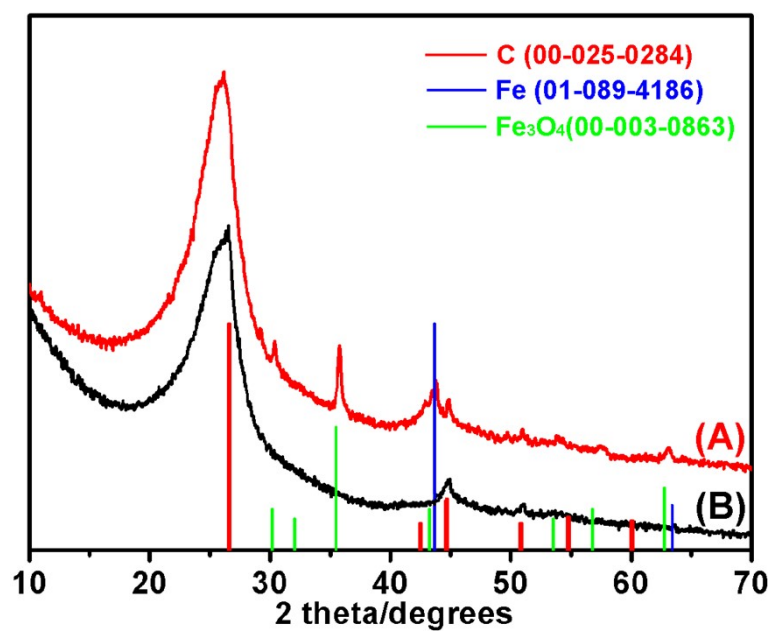


Figure S2. XRD pattern of (A) Fe/Fe₃O₄/NCNT and (B) NCNT array.

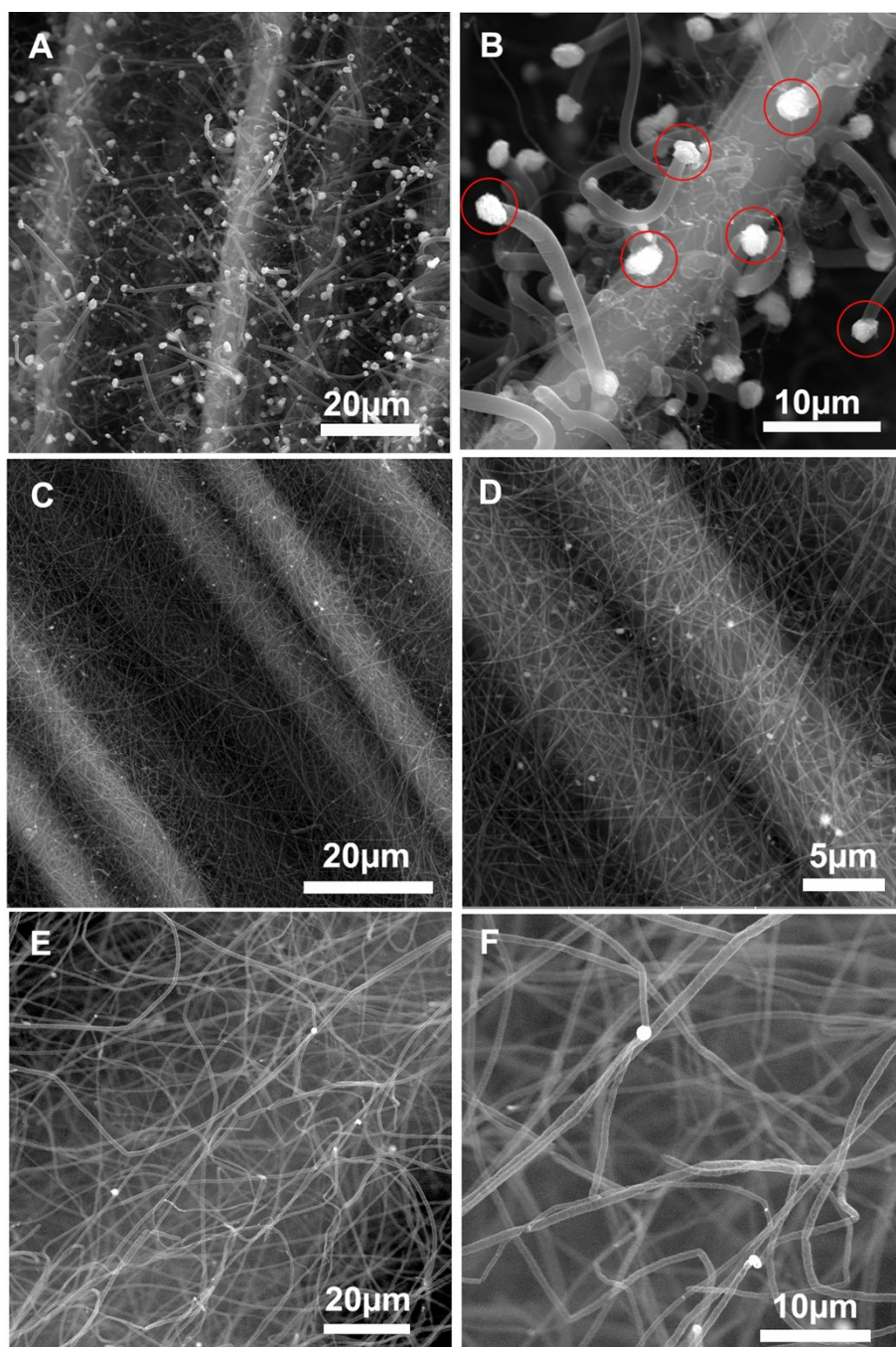


Figure S3. SEM images of Fe/Fe₃O₄/NCNT array formed after different pyrolysis times: (A, B) 10 min, (C, D) 30 min, and (E, F) 60 min.

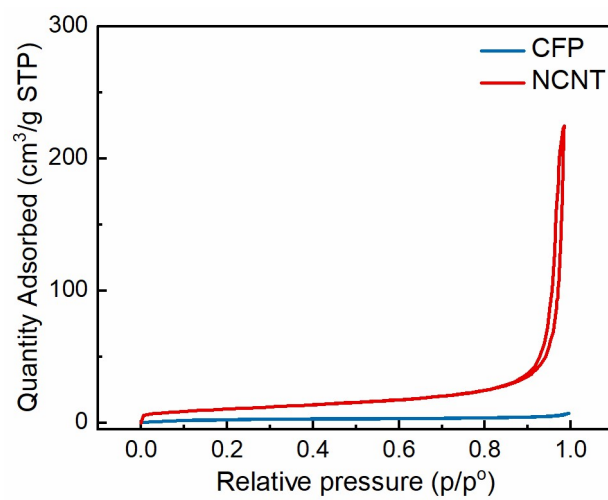


Figure S4. N₂ sorption isotherms of carbon fiber paper (CFP) and NCNT array.

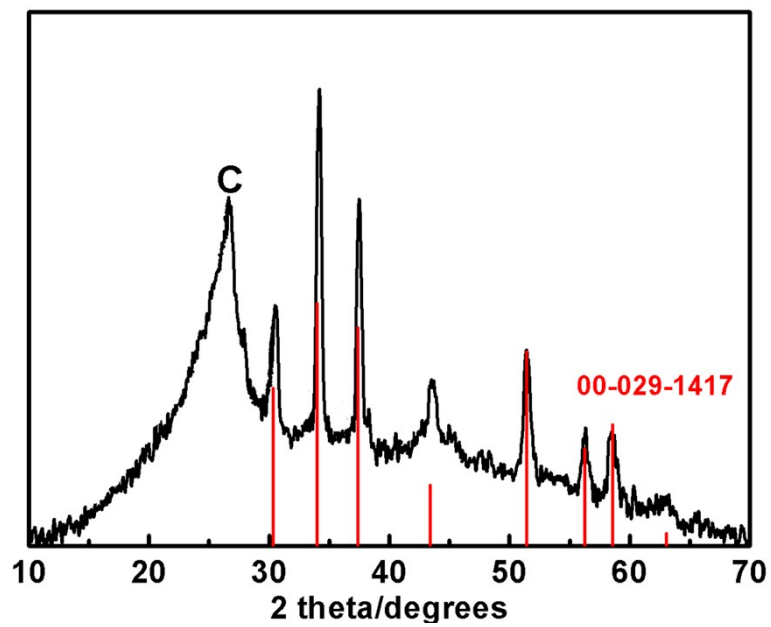


Figure S5. XRD pattern of $\text{Co}_{0.5}\text{Ni}_{0.5}\text{Se}_2/\text{NCNT}$, which is in consistent with the standard pattern of CoSe_2 (JCPDS 00-029-1417).

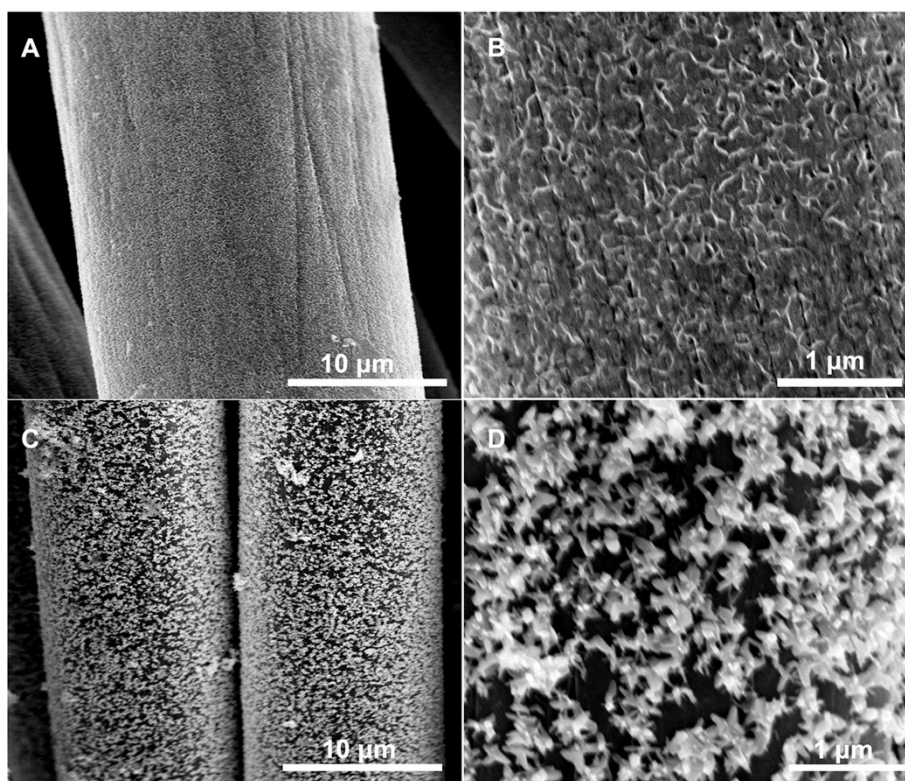


Figure S6. SEM images of (A, B) $\text{Co}_{0.5}\text{Ni}_{0.5}(\text{OH})_2/\text{CFP}$ and (C, D) $\text{Co}_{0.5}\text{Ni}_{0.5}\text{Se}_2/\text{CFP}$.

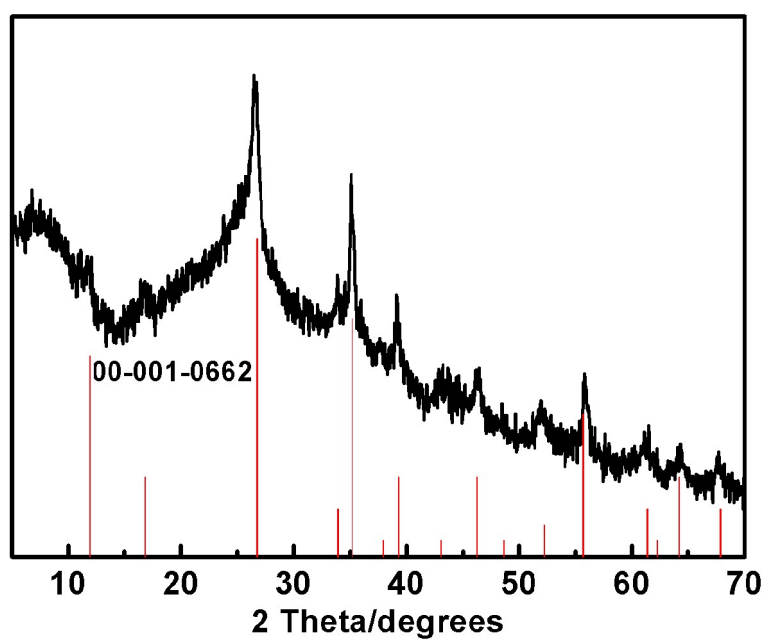


Figure S7. XRD pattern of the coaxial FeOOH/NCNT array, which is in accordance with the standard pattern of FeOOH (JCPDS 00-001-0662).

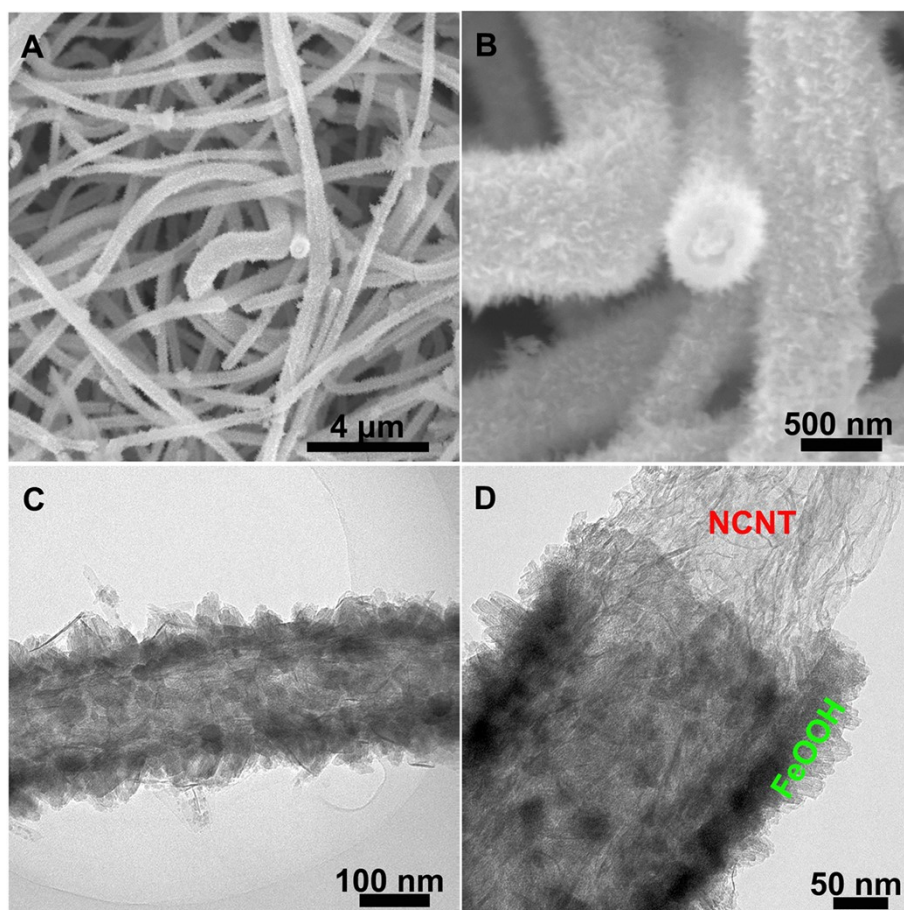


Figure S8. (A, B) SEM and (C, D) TEM images of the coaxial FeOOH/NCNT array.

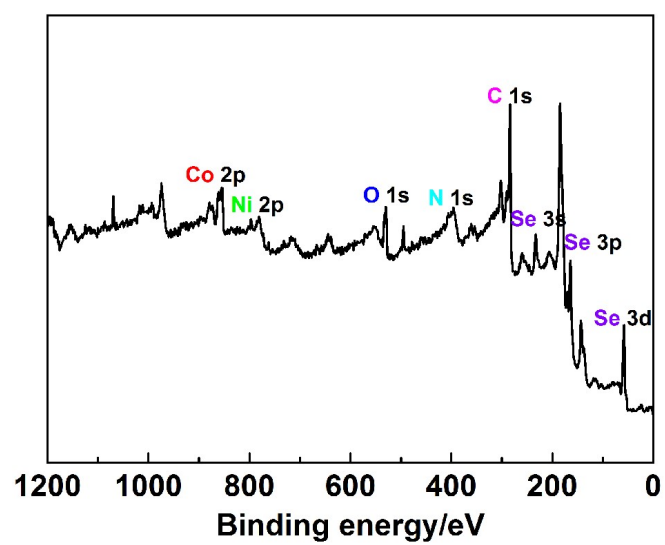


Figure S9. The XPS full spectrum of Co_{0.5}Ni_{0.5}Se₂/NCNT.

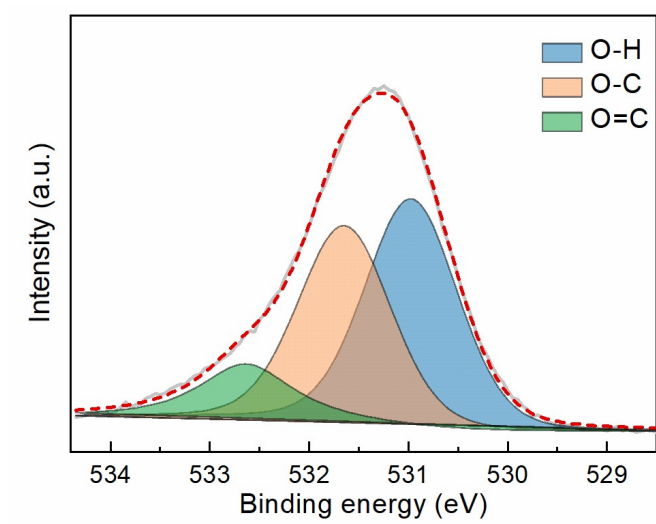


Figure S10. The O 1s XPS fine spectrum for Co_{0.5}Ni_{0.5}Se₂/NCNT.

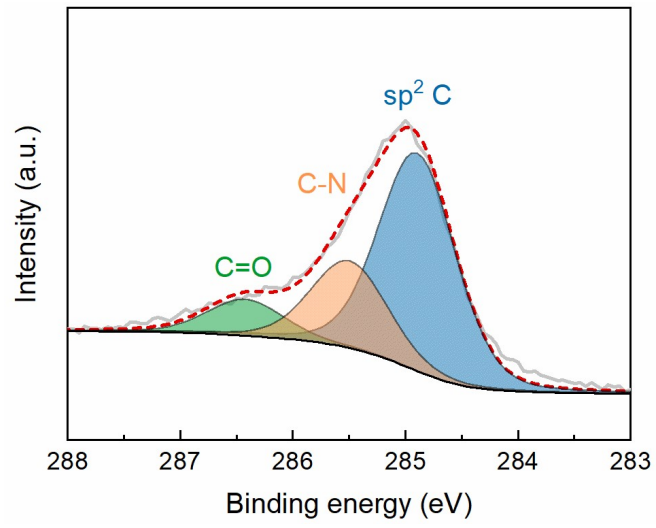


Figure S11. The C 1s XPS fine spectrum for Co_{0.5}Ni_{0.5}Se₂/NCNT.

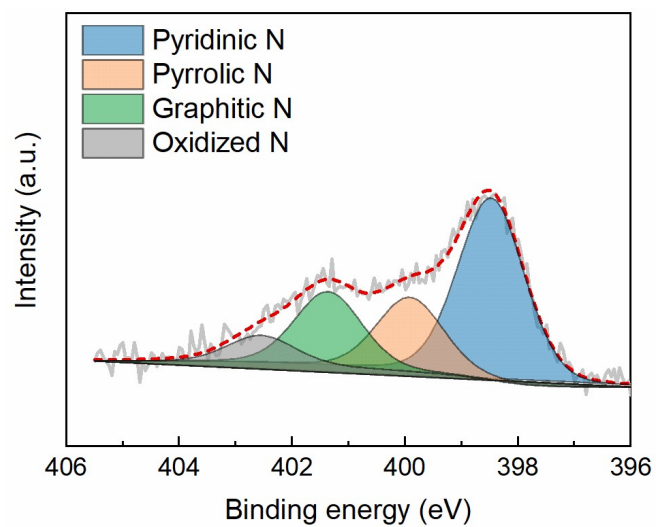


Figure S12. The N 1s XPS fine spectrum for Co_{0.5}Ni_{0.5}Se₂/NCNT.

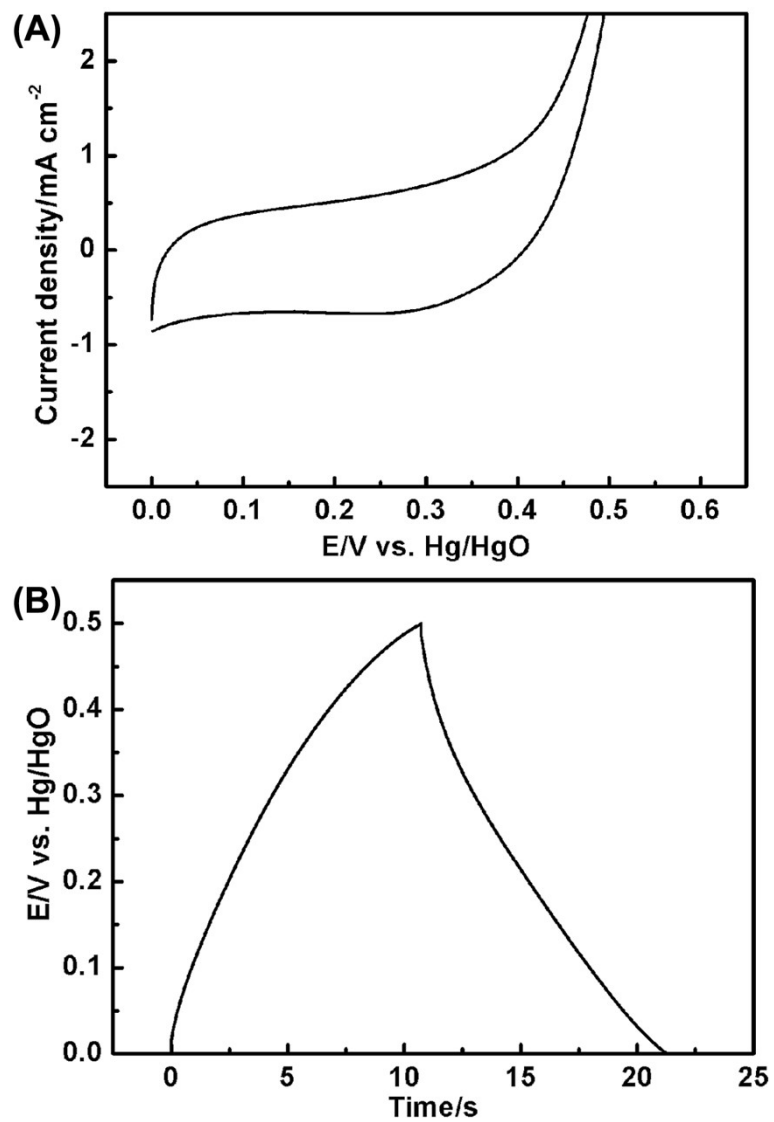


Figure S13. (A) CV curve (10 mV s^{-1}) and (B) galvanostatic charge/discharge curves at 4 mA cm^{-2} of NCNT. The areal capacity is 21.0 mC cm^{-2} at 4 mA cm^{-2} .

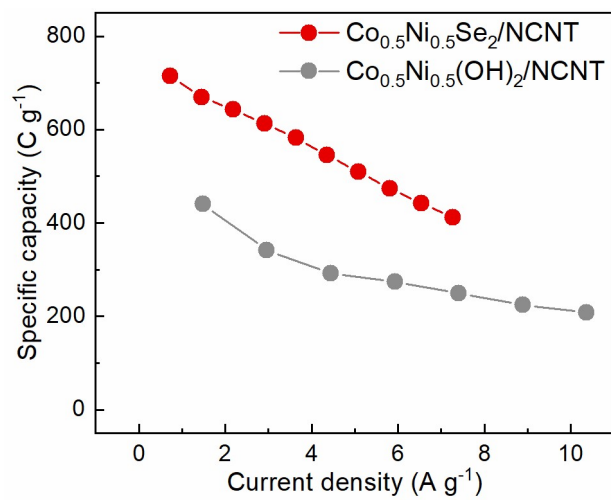


Figure S14. Specific capacity of Co_{0.5}Ni_{0.5}(OH)₂/NCNT and Co_{0.5}Ni_{0.5}Se₂/NCNT electrodes.

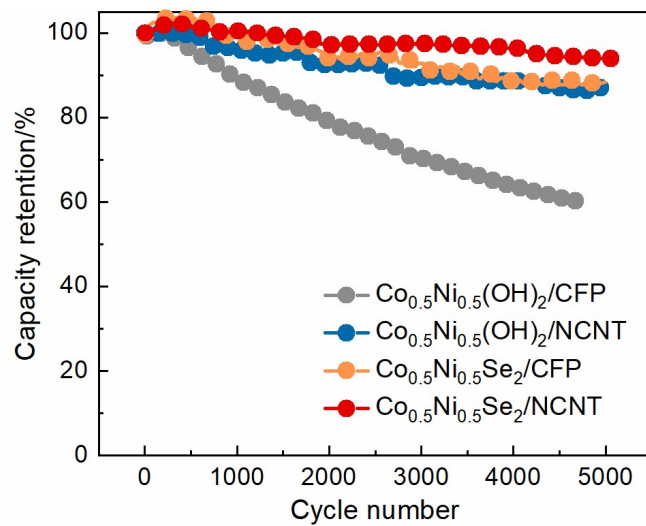


Figure S15. The long-term cycling performances of Co_{0.5}Ni_{0.5}(OH)₂/CFP, Co_{0.5}Ni_{0.5}(OH)₂/NCNT, Co_{0.5}Ni_{0.5}Se₂/CFP, and Co_{0.5}Ni_{0.5}Se₂/NCNT at a charging/discharging current of 20 mA cm⁻².

Table S1. Comparison of the specific capacity and rate capability of the $\text{Co}_{0.5}\text{Ni}_{0.5}\text{Se}_2/\text{NCNT}$ coaxial electrode with the Ni-Co-Se electrodes reported before.

Samples	Current density	Specific capacity	Rate capability	Ref.
$\text{Co}_{0.5}\text{Ni}_{0.5}\text{Se}_2/\text{NCNT}$	4.0 mA cm ⁻²	3.9 C cm ⁻² (714.5 C g ⁻¹)	57.6% (4-40)	This work
$\text{Ni}_{0.34}\text{Co}_{0.66}\text{Se}_2$	4.0 mA cm ⁻²	1.31 C cm ⁻²	75% (4-20)	1
Ni-Co-Se	1 A g ⁻¹	333.0 C g ⁻¹	40.6% (1-20)	2
Ni-Mn-Se	2 A g ⁻¹	1221.1 C g ⁻¹	78.8% (2-32)	3
$\text{NiCo}_{2.1}\text{Se}_{3.3}$	1 mA cm ⁻²	371.2 C g ⁻¹	63.5% (1-10)	4
NiCoSe_2	3 A g ⁻¹	375 C g ⁻¹	88.0% (3-10)	5
$(\text{Ni}_x\text{Co}_{1-x})_9\text{Se}_8$	5 A g ⁻¹	1692.9 C g ⁻¹	91.8% (5-30)	6
NiCoSe_4	0.5 A g ⁻¹	504 C g ⁻¹	85.2% (0.5-20)	7
$\text{Ni}_{0.5}\text{Co}_{0.5}\text{Se}_2$	1 A g ⁻¹	262 C g ⁻¹	56.0% (1-50)	8
$(\text{Ni}_{0.33}\text{Co}_{0.67})\text{Se}_2$	1 A g ⁻¹	414.0 C g ⁻¹	78.0% (1-30)	9
NiCoSe_2	1 A g ⁻¹	150.1 C g ⁻¹	63.3% (1-20)	10
NiCoSe_2	1 A g ⁻¹	520 C g ⁻¹	53.7% (1-30)	11

References

1. P. Xu, W. Zeng, S. Luo, C. Ling, J. Xiao, A. Zhou, Y. Sun and K. Liao, *Electrochim. Acta*, 2017, **241**, 41-49.
2. Y. L. Liu, C. Yan, G. G. Wang, F. Li, Q. Kang, H. Y. Zhang and J. C. Han, *Nanoscale*, 2020, **12**, 4040-4050.
3. A. Mohammadi Zardkhouhoui, B. Ameri and S. S. Hosseiny Davarani, *Nanoscale*, 2021, **13**, 2931-2945.
4. Y. Wang, W. Zhang, X. Guo, K. Jin, Z. Chen, Y. Liu, L. Yin, L. Li, K. Yin, L. Sun and Y. Zhao, *ACS Appl. Mater. Interfaces*, 2019, **11**, 7946-7953.
5. L. Hou, Y. Shi, C. Wu, Y. Zhang, Y. Ma, X. Sun, J. Sun, X. Zhang and C. Yuan, *Adv. Funct. Mater.*, 2018, **28**, 1705921.
6. P. Yang, Z. Wu, Y. Jiang, Z. Pan, W. Tian, L. Jiang and L. Hu, *Adv. Energy Mater.*, 2018, **8**, 1801392.
7. Z. Xie, D. Qiu, J. Xia, J. Wei, M. Li, F. Wang and R. Yang, *ACS Appl. Mater. Interfaces*, 2021, **13**, 12006-12015.
8. X. Song, C. Huang, Y. Qin, H. Li and H. C. Chen, *J. Mater. Chem. A*, 2018, **6**, 16205-16212.
9. L. Quan, T. Liu, M. Yi, Q. Chen, D. Cai and H. Zhan, *Electrochim. Acta*, 2018, **281**, 109-116.
10. Y. Miao, Y. Sui, D. Zhang, J. Qi, F. Wei, Q. Meng, Y. He, Z. Sun and Y. Ren, *Mater. Lett.*, 2019, **242**, 42-46.
11. L. Wang, Z. Feng, H. Zhang, D. Li and P. Xing, *Nanotechnology*, 2020, **31**, 125403.